DOI: 10.1002/ejic.200701015

Bridged Dinuclear Tripodal Tris(amido)phosphane Complexes of Titanium and Zirconium as Diligating Building Blocks for Organometallic Polymers

Hua Han[a] **and Samuel A. Johnson***[a]

Keywords: Tripodal ligands / Phosphane ligands / Titanium / Zirconium / Polymers

Appropriate bridging ligands allow for the preparation of bimetallic titanium and zirconium precursors to transition-metal-containing polymers using the formally trianionic $P(CH_2NAr^R)_3$ ligand (where Ar^R = Ph, and 3,5-$Me_2C_6H_3$ for **a** and **b**, respectively). Lithiation of the known amidophosphane ligand precursors $P(CH_2NHAr^R)_3$ (**1a**,**b**) with 3 equiv. of *n*BuLi cleanly provided the diethyl ether adducts $P(CH_2NAr^R)_3Li_3(OEt_2)_{1.5}$ (**2a**,**b**). The THF adduct $P(CH_2NPh)_3Li_3(THF)_5$ (**2a-THF**) was characterized by X-ray crystallography. Protonolysis reactions were used to prepare the mononuclear titanium complexes $P(CH_2NAr^R)_3TiOC_6H_4t\text{Bu}$ (**4a**,**b**) and dinuclear species $[P(CH_2NPh)_3TiNMe_2]_2$-μ-4,4′{O[3,3′,5,5′-$(C_6H_2Me_2)_2$]O} (**5a**), $[P(CH_2NPh)_3Ti]_2(\mu\text{-}O)$ (**6a**), and $P(CH_2N\text{-}3,5\text{-}Me_2C_6H_3)_3Ti\text{-}\mu\text{-}O\text{-}Ti(NMe_2)_3$ (**7b**), from $P(CH_2NAr^R)_3TiNMe_2$. The reactions of **1a**,**b** with $Zr(NEt_2)_4$ afforded metal complexes of the type $P(CH_2NAr^R)_3ZrNEt_2$ (**8a**,**b**). The chloride complexes $P(CH_2NAr^R)_3ZrCl(THF)$ (**9a**,**b**) were prepared by treatment of $HNEt_3Cl$ with **1** or **2**. The complexes **9a**,**b** reacted with cyclopentadienyllithium (C_5H_5Li) to produce $P(CH_2NAr^R)_3ZrCp$ (**10a**,**b**), which were also prepared by the reactions of the lithium salts **2a**,**b** with $CpZrCl_3$. The dilithium salt of the fulvalene dianion ($Li_2C_{10}H_8$) reacts with **9a**,**b** to produce the dinuclear complexes *trans*-$[P(CH_2NAr^R)_3Zr]_2(\mu\text{-}\eta^5{:}\eta^5\text{-}C_{10}H_8)$ (**10a**,**b**), respectively. The facile preparation of transition-metal-containing polymers from the bridged dinuclear complexes was illustrated by the reaction of **6a** with half an equivalent of $[Rh(CO)_2(\mu\text{-}Cl)]_2$, which precipitated polymeric $Cl(CO)Rh[P(CH_2NPh)_3Ti]_2(\mu\text{-}O)$.

Introduction

New methods to incorporate metal complexes into polymers or extended 2D and 3D structures are of current interest due to the additional physical properties, such as magnetism and redox chemistry, that the incorporation of these metal centers permits. A variety of methods have been used to incorporate metal centers in polymers or extended supramolecular networks,[1–3] which include the use of divergent diligating[4–10] donors incapable of coordinating to a single metal center.

Recently, we reported the synthesis and initial study of the tripodal amido phosphane ligands of the type $P(CH_2NHAr^R)_3$[11–13] where Ar^R is an aryl substituent. With metals in oxidation states greater than +3, these ligands preferentially form complexes where all three amido donors chelate to the metal, similar to other tripodal amido ligands.[14–16] Although the lone-pair of the phosphane donor is aimed away from the amido-chelated metal center, the minor lobe of this hybridized lone-pair orbital extends back towards the metal center. This through-space interaction[17] has been shown to influence the electronic parameter of this phosphane ligand,[12,18] and allows for the observation of through-space spin-spin coupling by NMR spectroscopy when the central metal is spin-active,[19] and in paramagnetic complexes provides an electronic exchange-coupling pathway when a second paramagnetic metal center is bound to the phosphane donor.[19] With suitable building blocks, this interaction could be used to create heterometallic[20,21] 1D wires, or 2D or 3D networks that could have properties resulting from through-space exchange-coupling, or through-space electron-transfer. The target bis(phosphane) building blocks for such an approach are shown in Scheme 1, and feature a pair of metal-bearing tripodal tris(amido)phosphane ligands, as well as a bridge between the metal centers labeled M. The addition of suitable late-transition-metal fragments capable of bonding to two phosphane moieties, labeled $M'L_n$ in Scheme 1, should provide a facile route to transition-metal-containing oligomers and polymers. Although there are a plethora of examples of bis(phosphanes) used as bridging ligands,[22–24] as well as flexible ligands incorporating hard and soft donors that have been utilized as building blocks for bimetallic and polynuclear early-late transition-metal clusters,[25,26] the complexes we propose here could provide rare examples of linear bis(phosphane) building blocks,[27–32] where through-space interactions provide the potential for extended interactions. In this paper, we test the synthetic feasibility of

---

[a] Department of Chemistry & Biochemistry, University of Windsor, Windsor, ON, Canada, N9B 3P4
E-mail: sjohnson@uwindsor.ca
Fax: +1-519-973-7098

preparing such building blocks using the diamagnetic early transition metals zirconium and titanium, with the goal of introducing redox active and paramagnetic metal-bridge fragments in future endeavours.

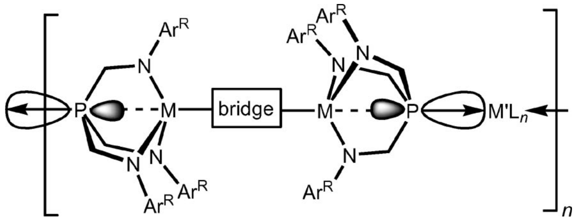

Scheme 1.

Results and Discussion

The reaction of lithium salts of amido donors with transition-metal chlorides is a typical route to transition-metal ancillary ligand complexes, and thus the lithium salts of $P(CH_2NHAr^R)_3$ (**1a**,**b**) were sought after as useful precursors (where the aromatic substituents, Ar^R = Ph and 3,5-$Me_2C_6H_3$ are denoted as **a** and **b**, respectively). The lithium salt of the phenyl-substituent-bearing ligands were easily obtained by the reaction of a slurry of $P(CH_2NHPh)_3$ in diethyl ether with 3 equiv. of *n*BuLi, as shown in Scheme 2. After the addition of 2 equiv. of *n*BuLi the solids dissolved, and the addition of the 3rd equiv. resulted in the precipitation of the analytically pure product, $P(CH_2NPh)_3Li_3(OEt_2)_{1.5}$ (**2a**). The lithium salt $P(CH_2N\text{-}3,5\text{-}Me_2C_6H_3)_3Li_3(OEt_2)_{1.5}$ (**2b**) was prepared in an analogous manner from **1b**. The complexes **2a** and **2b** are insoluble in toluene, diethyl ether and dichloromethane, but soluble in THF. The dissolution of THF results in the displacement of the diethyl ether donors as demonstrated by the crystallization of $P(CH_2NPh)_3Li_3(THF)_5$ (**2a-THF**) by cooling a THF solution of **2a**. This THF adduct is soluble in cold CH_2Cl_2, but decomposes over the course of 1 h at room temperature in this solvent.

$$\underset{\textbf{1a}}{P(CH_2NHPh)_3} \xrightarrow[Et_2O]{+3\ n\text{BuLi}} \underset{\textbf{2a}}{P(CH_2NPh)_3Li_3(OEt_2)_{1.5}}$$

$$\xrightarrow{THF} \underset{\textbf{2a-THF}}{P(CH_2NPh)_3Li_3(OC_4H_8)_5}$$

$$\underset{\textbf{1b}}{P(CH_2NH\text{-}3,5\text{-}Me_2C_6H_3)_3} \xrightarrow[Et_2O]{+3\ n\text{BuLi}}$$

$$\underset{\textbf{2b}}{P(CH_2N\text{-}3,5\text{-}Me_2C_6H_3)_3Li_3(OEt_2)_{1.5}}$$

Scheme 2.

The solid-state molecular structure of **2a-THF** was determined by X-ray crystallography and is shown in Figure 1. The complex has an approximate mirror plane of symmetry, with the central Li ion, Li(3), chelated by all three amido donors and bearing a single THF donor. The two remaining Li ions bridge between amido donors, and adopt four-coordinate geometries by bonding to two THF moieties apiece. Lithium salts of tripodal amido donors are known to adopt a multitude of bonding motifs in the solid state,[33] and structurally related tripodal amido lithium salts are known.[34]

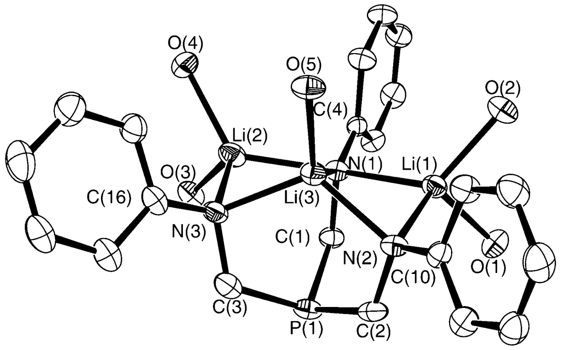

Figure 1. Solid-state molecular structure of **2a-THF** as determined by X-ray crystallography. Ellipsoids are shown at the 33% probability level. Hydrogen atoms are omitted and only the oxygen atoms associated with the THF donors are shown for clarity. Selected distances [Å]: Li(1)–N(2) 2.069(7), Li(1)–N(1) 2.189(8), Li(2)–N(1) 2.150(9), Li(2)–N(3) 2.053(7), Li(3)–N(3) 2.063(7), Li(3)–N(2) 2.088(7), Li(3)–N(1) 2.149(7), Li(3)–P(1) 3.074(6). Selected bond angles (°): C(2)–P(1)–C(1) 104.38(18), C(2)–P(1)–C(3) 101.5(2), C(1)–P(1)–C(3) 107.84(19).

The room temperature ^1H, ^7Li, and $^{13}C\{^1H\}$ NMR spectra of both **2a** and **2b** are consistent with high symmetry species. The ^1H NMR spectrum of **2a** in [D$_8$]THF consists of a single PCH_2 resonance and a set of three aromatic resonances, and the ^7Li NMR spectrum displays a single lithium environment. The fluxional nature of Li salts of related species is well documented.[34] The $^{31}P\{^1H\}$ NMR spectrum of **2a** and **2b** in [D$_8$]THF display singlets at δ = –22.2 and –21.7 ppm, respectively, which are only slightly altered from the δ = –32.1 and –29.6 ppm chemical shifts observed for **1a** and **1b**. The change of shift is in the opposite direction we have previously observed for early transition-metal complexes of these ligands, which exhibit ^{31}P chemical shifts as low as –108.5 ppm.[12]

Synthesis and Characterization of Titanium Complexes

A variety of synthetic approaches to $P(CH_2NAr^R)_3TiCl$ were attempted, due to the fact that it could serve as a potential precursor to a variety of bridged dinuclear complexes via salt metathesis. Unfortunately, the direct reaction of the lithium salts **2a**,**b** with $TiCl_4$ produced a mixture of products. The reaction of the ligand precursors $P(CH_2NHAr^R)_3$ with stoichiometric quantities of $(Me_2N)_3$-

TiCl also failed to produce the desired product, and the previously characterized $P(CH_2NAr^R)_3TiNMe_2$[12] and unreacted $P(CH_2NHAr^R)_3$ were identified as two of the major components of the reaction mixture in each case. Similarly, the reaction of $P(CH_2NAr^R)_3TiNMe_2$ with either the ammonium salt $HNEt_3Cl$, or Me_3SiCl, failed to yield the desired chloride complex.

Due to the difficulty in accessing the chloride complex, we attempted to demonstrate that the amido complexes, $P(CH_2NAr^R)_3TiNMe_2$ (**3a**,**b**), could act as precursors to bridged complexes through protonolysis reactions. To test this hypothesis we prepared the mononuclear complexes $P(CH_2NAr^R)_3TiOC_6H_4t$Bu (**4a**,**b**) by the reaction of 1,4-HOC_6H_4tBu with $P(CH_2NAr^R)_3TiNMe_2$ in toluene, as shown in Equation (1). The reactions are slow at room temperature, and required 48 h to go to completion. The resultant products are thermally stable dark-red solids.

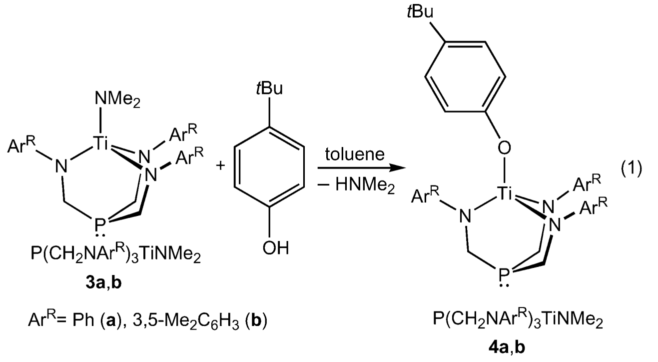

Crystalline **4b** was obtained by slow evaporation of a pentane solution, and the solid-state molecular structure was determined by X-ray crystallography. The unit cells contain two crystallographically distinct molecules of **4b** in the asymmetric unit, and an ORTEP depiction of one of these is shown in Figure 2. The four-coordinate structure is a distorted tetrahedron, with the phosphane lone pair formally directed away from the titanium center. The Ti(1)–O(1)–C(28) bond angle of 160.20(3)° is distorted significantly from linearity, but this angle and the Ti–O distance of 1.784(3) Å are typical.[35] The Ti–N bonds of **4b** [1.918(4), 1.918(4), 1.926(4) Å] are shorter than those of $P(CH_2N\text{-}3,5\text{-}Me_2C_6H_3)TiNMe_2$ (**3b**) [1.963(7), 1.941(6), 1.934(6) Å], reflecting the slightly stronger σ-bonding and π-donation from these donors in compound **4b**.[36] The $^{13}C\{^1H\}$ NMR chemical shift of the *ipso* carbon atoms bonded directly to the oxygen atoms are at δ = 164.2 and 153.3 ppm, for **4a** and **4b**, respectively, which reflects how strongly the degree of π-donation from the oxygen donor in these complexes is influenced by the amido donor substituents.[35] The sum of C–P–C bond angles and P···Ti distances in the solid-state structure of complex **4b** are similar to those observed in the parent compound $P(CH_2N\text{-}3,5\text{-}Me_2C_6H_3)_3TiNMe_2$ (**3b**); however, the $^{31}P\{^1H\}$ NMR chemical shifts in **4a**,**b** of δ = –81.1 and –77.9 ppm, respectively, are significantly different than those of **3a**,**b**, which are δ = –65.6 and –61.6 ppm. This corroborates our previous observation that the electron density at the chelated metal center affects the properties of the phosphane donor, despite the fact that the phosphane lone-pair is not coordinated to the metal center.[12]

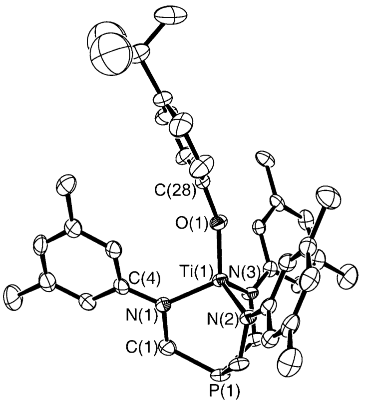

Figure 2. Solid-state molecular structure of **4b** as determined by X-ray crystallography. Ellipsoids are shown at the 50% probability level. Hydrogen atoms are omitted for clarity. Selected distances [Å]: Ti(1)···P(1) 3.0150(16), Ti(1)–N(1) 1.918(4), Ti(1)–N(2) 1.926(4), Ti(1)–N(3) 1.918(4), Ti(1)–O(1) 1.784(3), O(1)–C(28) 1.369(5), P(1)–C(1) 1.854(5), P(1)–C(2) 1.861(5), P(1)–C(3) 1.863(5). Selected bond angles: O(1)–Ti(1)–P(1) 178.20(12), Ti(1)–O(1)–C(28) 160.20(3), C(1)–P(1)–C(2) 102.8(2), C(1)–P(1)–C(3) 102.8(2), C(2)–P(1)–C(3) 102.8(2), N(1)–Ti(1)–O(1) 112.66(16), N(2)–Ti(1)–O(1) 115.74(16), N(3)–Ti(1)–O(1) 113.82(16), N(1)–Ti(1)–N(3) 105.73(17), N(2)–Ti(1)–N(3) 104.02(16), N(2)–Ti(1)–N(1) 103.77(16).

Aryloxy ligands have been utilized in the past as bridging ligands to generate binuclear or larger complexes with cyclopentadienyl-substituted titanium and zirconium complexes.[35,37,38] The reaction of 4,4′-HO[3,3′,5,5′-$(C_6H_2Me_2)_2$]OH with 2 equiv. $P(CH_2NPh)_3TiNMe_2$ (**3a**) in toluene is slow at room temperature, and after 48 h gave the binuclear compound $[P(CH_2NPh)_3Ti]_2$\{μ-O[3,3′,5,5′-$(Me_2C_6H_2)_2$]O-\} (**5a**) as a red solid in 85% yield, as shown in Equation (2). Compound **5a** is soluble in aromatic hydrocarbons such as toluene and benzene. The ^1H NMR and $^{13}C\{^1H\}$ NMR spectra of compound **5a** show the disappearance of $–NMe_2$ ligand and equivalence of the two Ti

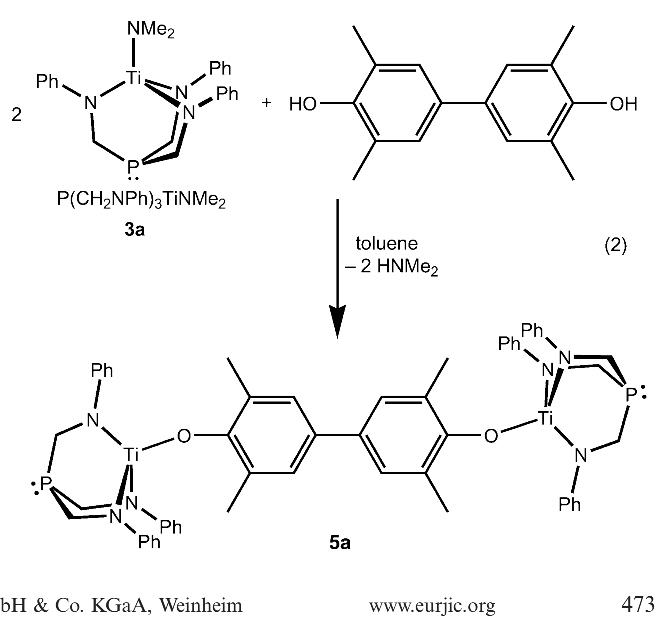

metal fragments, as well as one set of aromatic resonances. In the ^{1}H NMR spectrum, the aromatic protons of the {μ-O[3,3′,5,5′-($C_6H_2Me_2$)$_2$]O-}$^{2-}$ ligand are equivalent and appear as a singlet at δ = 7.17 ppm. The ^{31}P{^{1}H} NMR spectrum displays a singlet at δ = –78.6, which is comparable to that of $P(CH_2NPh)_3TiOC_6H_4tBu$ (**4a**) at δ = –81.1 ppm. Unfortunately, the analogous complex **5b** could not be prepared by this method, and attempts to prepare crystals of **5a** suitable for study by X-ray diffraction only generated a microcrystalline solid.

Single atom oxo-bridges are also accessible, though not by direct reaction with H_2O.[39] The reaction of $P(CH_2NPh)_3TiNMe_2$ (**3a**) with 1/2 an equivalent of H_2O results in an insoluble colorless precipitate that likely consists largely of TiO_2. However, the slow addition of a stoichiometric amount of water by using the hydrated salt $Na_2SO_4 \cdot 10H_2O$ resulted in the formation of the oxo-bridged binuclear compound $[P(CH_2NPh)_3Ti]_2(\mu\text{-}O)$ (**6a**), as shown in Equation (3).

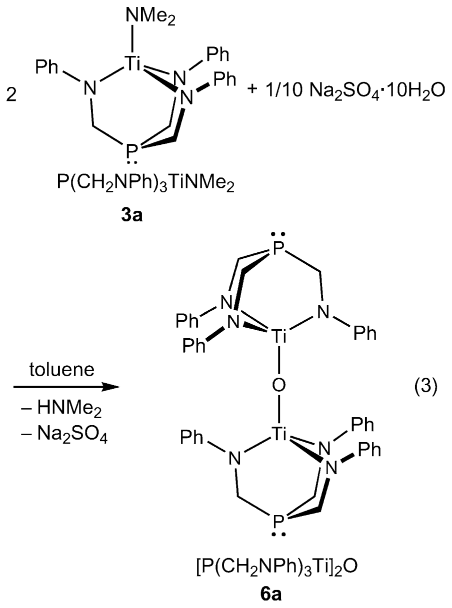

(3)

The bridging oxo formulation was confirmed by X-ray crystallography, and an ORTEP depiction of the solid-state molecular structure is shown in Figure 3. Complex **6a** crystallizes from toluene to give crystals belonging to the trigonal space group and possessing the crystallographically imposed S_6 symmetry. A second monoclinic pseudopolymorph containing cocrystallized toluene was also characterized; however, no significant structural differences were observed. The molecule has a strictly linear P–Ti–O–Ti–P unit, which defines the S_6 axis. As expected, the ^{1}H NMR spectrum of **6a** contains only the PCH_2 and three aromatic resonances associated with the ancillary ligand. The ^{31}P{^{1}H} NMR shift of –39.3 ppm is unusual, compared to the chemical shift of **4a** and **5a**, which are more negative by almost 40 ppm. A reasonable rationale for this shift might be that the steric interaction between the two ancillary ligand moieties in **6a** result in a strained ligand conformation with larger N–Ti–O angles and P–Ti distances. The bond angles and lengths corroborate this hypothesis. For example, the Ti(1)···P(1) separation of 3.051(2) Å is the longest we have observed in Ti complexes of these ancillary ligands.

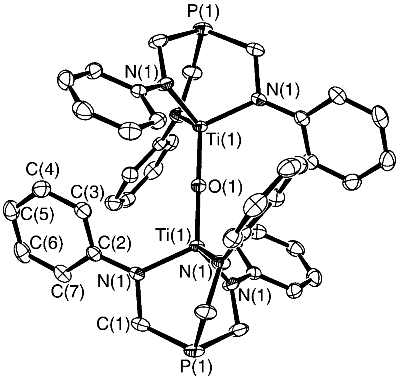

Figure 3. Solid-state molecular structure of **6a** as determined by X-ray crystallography. Ellipsoids are shown at the 50% probability level. Hydrogen atoms are omitted for clarity. Selected distances [Å]: Ti(1)···P(1) 3.051(2), Ti(1)–N(1) 1.907(2), Ti(1)–O(1) 1.802(8), C(1)–P(1) 1.855(3), C(1)–N(1) 1.467(4), C(2)–N(1) 1.397(3), Selected bond angles: P(1)–Ti(1)–O(1)–Ti(2) 180.00(0), N(1)–Ti(1)–O(1) 115.46(7), N(1)–C(1)–P(2) 115.53(2), C(1)–N(1)–C(2) 118.29(2), C(2)–N(1)–Ti(1) 129.96(18), C(1)–N(1)–Ti(1) 110.61(18), C(1)–P(1)–C(1) 102.05(11).

Attempts to make an analogous bridging oxo complex with $P(CH_2N\text{-}3,5\text{-}Me_2C_6H_3)_3TiNMe_2$ (**3b**) have failed, possibly due to the steric bulk afforded by the aromatic methyl substituents; however, it may be that kinetic factors prevent its facile preparation. In an attempt to find an alternate route to these complexes, compound **3b** was treated with 1 equiv. of H_2O and excess $Ti(NMe_2)_4$ at room temperature to yield the binuclear titanium complex $P(CH_2N\text{-}3,5\text{-}Me_2C_6H_3)_3Ti\text{-}\mu\text{-}O\text{–}Ti(NMe_2)_3$ (**7b**), as shown in Equation (4). Crystals suitable for an X-ray structure analysis

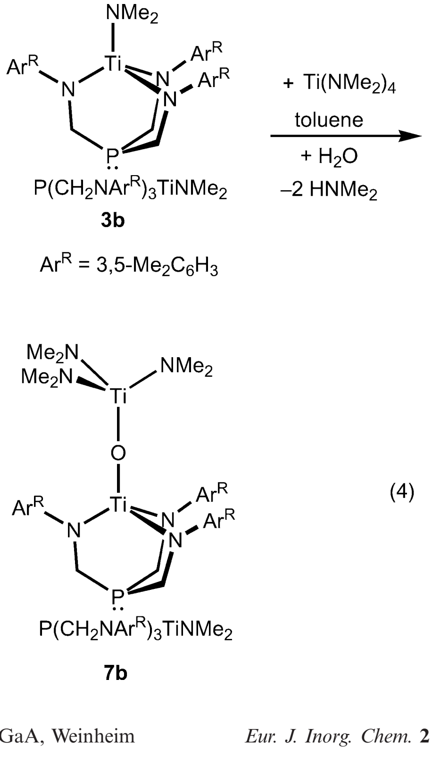

(4)

were grown by slow evaporation of a toluene solution at –30 °C. Unfortunately, attempts to react **7b** with $P(CH_2NH\text{-}3,5\text{-}Me_2C_6H_3)_3$ failed to produce the desired product, $[P(CH_2N\text{-}3,5\text{-}Me_2C_6H_3)_3Ti]_2(\mu\text{-}O)$.

Figure 4 shows the solid-state molecular structure of **7b**, as well as the selected bond lengths and bond angles. The binuclear compound of **7b** crystallizes in the rhombohedral space group *R*-3, and the molecular structure has crystallographically imposed C_3 symmetry. Both titanium atoms are connected by a linear μ-oxo bridge, and the Ti(1)–O(1) bond length of 1.757(3) Å is shorter than Ti(2)–O(1) bond length of 1.886(3) Å. This is likely due to significantly greater π-donation by the O-donor to Ti(1).[40] The aromatic substituents render the ancillary ligand amido donors less potent than the $\text{-}NMe_2$ groups, but also the hindered rotation of the chelating amido donors prevents optimal overlap of these orbitals with the available d orbitals on Ti(1). The Ti(1)···P(1) distance of 2.968(14) Å is just slightly shorter than observed for **3b** or **4b**, 3.015(5) and 3.015(16) Å, respectively. Also noteworthy is the $^{31}P\{^1H\}$ NMR shift of $\delta = -62.9$, which is significantly different than the shift of –39.4 observed for **6a**.

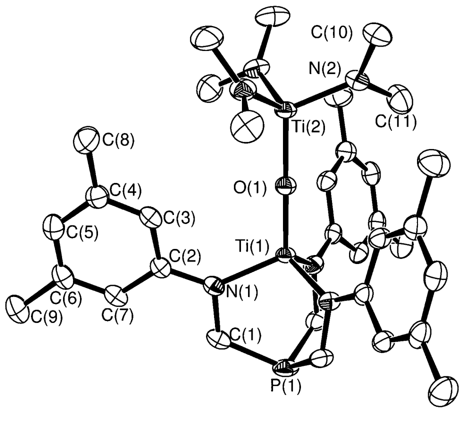

Figure 4. Solid-state molecular structure of **7b** as determined by X-ray crystallography. Ellipsoids are shown at the 50% probability level. Hydrogen atoms are omitted for clarity. Selected distances [Å]: Ti(1)···P(1) 2.968(14), Ti(1)–N(1) 1.935(2), Ti(1)–O(1) 1.757(3), Ti(2)···P(1) 6.612, Ti(2)–N(2) 1.881(2), Ti(2)–O(1) 1.886(3), C(1)–P(1) 1.850(3), C(1)–N(1) 1.461(3), Selected bond angles: Ti(1)–O(1)–Ti(2) 180.0, N(1)–Ti(1)–N(1) 106.15(7), N(1)–Ti(1)–O(1) 112.62(6), N(2)–Ti(2)–N(2) 105.13(8), N(2)–Ti(2)–O(1) 113.52(7), C(1)–P(1)–C(1) 103.65(10), C(1)–N(1)–C(2) 115.74(2), C(1)–N(1)–Ti(1) 108.01(16), C(2)–N(1)–Ti(1) 135.87(16), C(10)–N(2)–C(11) 112.45(2), C(10)–N(2)–Ti(2) 129.37(2), C(11)–N(2)–Ti(2) 117.99(18).

Synthesis and Characterization of Zirconium Complexes

Similar to the Ti complexes, attempts to react $ZrCl_4(THF)_2$ with the lithium salts **2a**,**b** under a variety of reaction conditions produced only trace amounts of the complex $P(CH_2NAr^R)_3ZrCl(THF)$, identifiable in the $^{31}P\{^1H\}$ NMR due to its later preparation by an alternate route (vide infra). The reaction of phosphane ligands $P(CH_2NHAr^R)_3$[12] with 1 equiv. $Zr(NEt_2)_4$ cleanly produced the mononuclear zirconium complexes $P(CH_2NAr^R)_3ZrNEt_2$ (**8a**,**b**) with the concomitant elimination of 3 equiv. of $HNEt_2$, as shown in Scheme 3.

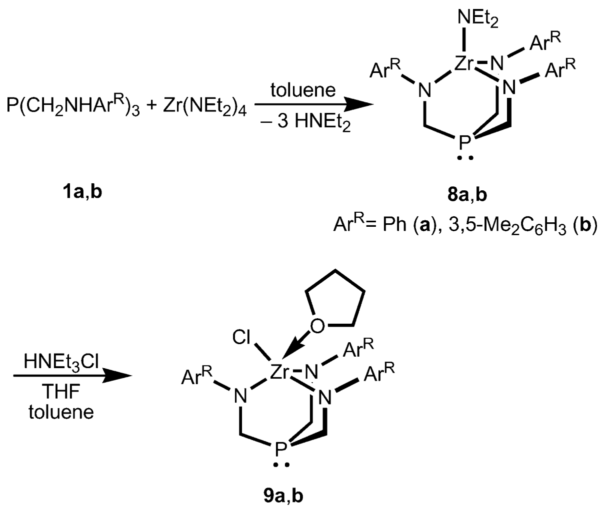

Scheme 3.

These reactions require 24–48 h to go to completion and no intermediates were observed by ^1H or $^{31}P\{^1H\}$ NMR spectroscopy. The resultant products are all obtained in 69–86% yields as thermally stable yellow solids. The room-temperature ^1H NMR spectra ([D$_6$]benzene) of $P(CH_2NAr^R)_3ZrNEt_2$ (**8a**,**b**) correspond to apparent threefold symmetric complexes in solution, similar to the structurally characterized $P(CH_2NAr^R)_3TiNMe_2$ (**3a**,**b**). The monomeric formulations of the solution structures were verified by measuring the diffusion rates of $P(CH_2NAr^R)_3ZrNEt_2$ (**8a**,**b**) by diffusion-ordered NMR spectroscopy (DOSY NMR). The rates proved to be nearly identical to the complexes **3a** and **3b**.

The $^{31}P\{^1H\}$ chemical shifts are $\delta = -75.2$ and –70.8 ppm for **8a**,**b**, respectively. These values are significantly more negative than those of the Ti analogues, and opposite to the expected shift due to the increase of C–P–C angles that results from the ligand straining to accommodate a much larger Zr metal center. These shifts provide additional evidence that an electrostatic through-space interaction strongly affects the phosphane moiety in these complexes.[12]

The zirconium chloride complexes $P(CH_2NAr^R)_3ZrCl(THF)$ (**9a**,**b**) were readily prepared by reaction of $P(CH_2NAr^R)_3ZrNEt_2$ (**8a**,**b**) with $HNEt_3Cl$, and isolated in 84.1–89.6% yields as yellow solids. The reaction was carried out in toluene at room temperature. After 1 h, THF was added just before the solvent was removed. If the solvent was removed without first adding THF, the product decomposed. The chloride complex formed in the absence of THF is likely stabilized by $HNEt_2$, which is removed under vacuum. When the reaction of $P(CH_2NAr^R)_3ZrNEt_2$ (**8a**,**b**) with $HNEt_3Cl$ was performed using THF as the solvent, it took more than 48 h to go to completion and a plethora of long-lived intermediates were observed by $^{31}P\{^1H\}$ NMR spectroscopy. This probably indicates that the amido donors of the tridentate ligands are protonated as easily as diethylamido ligand, and the THF solvent molecules can then coordinate to the zirconium metal center and block proton-transfer pathways, thus rendering the formation of the thermodynamic products slow.

The $^{31}P\{^1H\}$ NMR chemical shifts for $P(CH_2NAr^R)_3ZrCl(THF)$ (**9a**,**b**) are $\delta = -71.5$ and -66.0 ppm, respectively. The room-temperature ^1H NMR spectra are consistent with the presence of 1 equiv. coordinated THF. Despite apparent five-coordinate geometries, **9a**,**b** both exhibit ^1H and $^{13}C\{^1H\}$ NMR spectra that are consistent with threefold pseudosymmetry in solution. Attempts to gain insight into the nature of the fluxional process required for such apparent symmetry were made by monitoring the ^1H spectra of $[D_8]$toluene solutions of **9a**,**b** down to –80 °C, but no broadening or decoalescence of resonances were observed. The diffusion rates of the complexes $P(CH_2NAr^R)_3ZrNEt_2$ (**8a**,**b**) and **9a**,**b**, were obtained by diffusion-ordered NMR spectra (DOSY NMR) and were found to be nearly identical; although it is notable that the resonances associated with the coordinated THF moieties of **9a**,**b** diffused at a slightly faster rate, indicative of rapid dissociation and association in solution. Consistent with this observation, the addition of THF to C_6D_6 solutions of **9a**,**b** resulted in a pair of shifted resonances, rather than unique pairs of resonances for coordinated and free THF molecules.

Attempts to make the hydride, methyl, or benzyl-substituted complexes from the reaction of the zirconium chloride precursor **9a**,**b** with NaH, MeLi, or $BrMgCH_2Ph$ all failed. The latter complex could also not be prepared by the reaction of the $P(CH_2NHAr^R)_3$ ligand precursors with $Zr(CH_2Ph)_4$. Similarly, attempts to make aryloxy species similar to those prepared with the titanium complexes failed, either by protonolysis reactions using **8a**,**b**, or salt metathesis reactions using **9a**,**b**. It appears that these relatively coordinatively unsaturated complexes are too unstable to isolate; however, the reaction of $P(CH_2NAr^R)_3ZrCl(THF)$ with CpLi (where Cp = C_5H_5) produced the cyclopentadienyl complex $P(CH_2NAr^R)_3ZrCp$, as shown in Scheme 4. The reaction of the lithium salts **2a**,**b** with $CpZrCl_3$ provides an alternate route to these complexes.

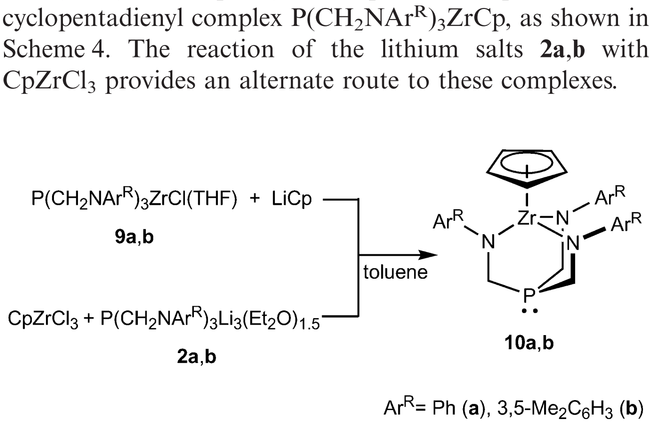

Scheme 4.

X-ray-quality single crystals of **10b** were obtained from the slow evaporation of a saturated toluene solution, and the solid-state molecular structure is depicted in Figure 5. As anticipated, the structure reveals an η^5-coordinated cyclopentadienyl ligand in the coordination pocket of the trisamido-chelated $P(CH_2NAr^R)_3Zr$ fragment. The sum of C–P–C angles in 316.0(2)° is larger than observed in any of the titanium complexes, consistent with the strain on the ancillary ligand to accommodate a large metal such as Zr. The Zr(1)···P(1) separation of 3.0523(6) Å is only slightly longer than typical Zr–P bond lengths, which reside between 2.7–2.9 Å, and is nearly identical to the longest reported Zr–P bond length of 3.033 Å, which was observed in an organometallic PMe_3 adduct.[41]

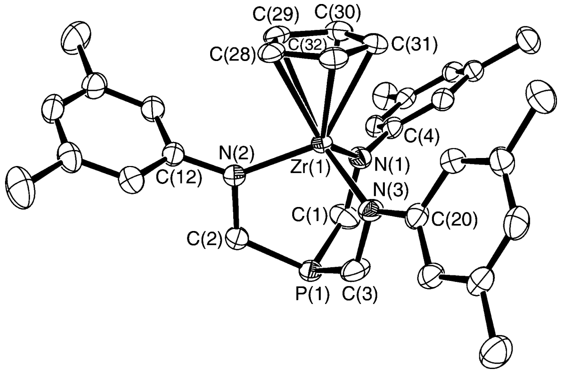

Figure 5. Solid-state molecular structure of **10b** as determined by X-ray crystallography. Ellipsoids are shown at the 50% probability level. Hydrogen atoms are omitted for clarity. Selected distances [Å]: Zr(1)···P(1) 3.0523(6), Zr(1)–N(1) 2.0536(18), Zr(1)–N(2) 2.0624(17), Zr(1)–N(3) 2.0986(17), Zr(1)–C(28) 2.5290(19), Zr(1)–C(29) 2.553(2), Zr(1)–C(30) 2.541(2), Zr(1)–C(31) 2.518(2), Zr(1)–C(32) 2.498(2), P(1)–C(1) 1.850(2), P(1)–C(2) 1.846(2), P(1)–C(3) 1.857(2). Selected bond angles: C(1)–P(1)–C(2) 104.93(12), C(1)–P(1)–C(3) 106.40(12), C(2)–P(1)–C(3) 104.66(11), Zr(1)–N(1)–C(1) 107.31(13), Zr(1)–N(1)–C(4) 139.05(14), Zr(1)–N(2)–C(2) 109.55(13), Zr(1)–N(2)–C(12) 137.95(14), Zr(1)–N(3)–C(3) 105.76(13), Zr(1)–N(3)–C(20) 140.52(14), P(1)–C(1)–N(1) 120.31(16), P(1)–C(2)–N(2) 118.48(15), P(1)–C(3)–N(3), 121.69(16), C(1)–N(1)–C(4) 113.62(17), C(2)–N(2)–C(12) 112.46(16), C(3)–N(3)–C(20) 113.60(17), N(1)–Zr(1)–N(2) 104.91(7), N(1)–Zr(1)–N(3) 99.37(7), N(2)–Zr(1)–N(3) 106.38(7).

The stability of the cyclopentadienyl zirconium complexes **10a**,**b** suggests that the most versatile dinuclear zirconium building blocks should bear polyhapto ligands. The fulvalene dianion $(C_{10}H_8)^{2-}$ has been used as a bridging ligand to promote intermetal communication,[42–47] and its obvious relation to the Cp ligand suggested that these complexes should be stable and isolable. The reactions of 2 equiv. of $P(CH_2NAr^R)_3ZrCl(THF)$ (**9a**,**b**) with 1 equiv. of $(C_{10}H_8)Li_2$[48] at room temperature provided the binuclear zirconium complexes *trans*-$[P(CH_2NAr^R)_3Zr]_2(\eta^5{:}\eta^5\text{-}C_{10}H_8)$ (**11a**,**b**), as shown in Equation (5). These hydrocarbon-soluble complexes were purified by slow evaporation of saturated benzene/hexamethyldisiloxane solutions, which provided yellow crystalline solids.

The structure of compound **11b** was confirmed by X-ray diffraction and an ORTEP depiction of the solid-state molecular structure is shown in Figure 6, together with selected bond lengths. The molecule crystallizes with a center of symmetry; the two metal centers are crystallographically

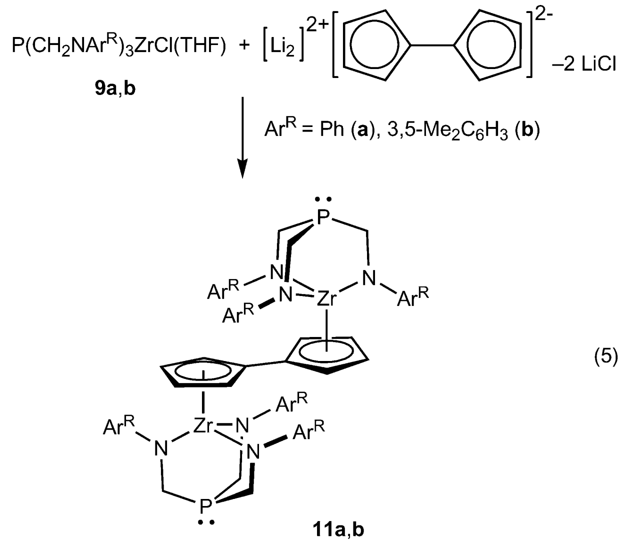

11a,b

(5)

equivalent and are coordinated to the bridging fulvalenide ligand in a *trans* manner.[49] Both ^{1}H and ^{31}P{^{1}H} NMR spectroscopy support the presence of only the *trans* isomer; the ^{31}P{^{1}H} NMR spectra of complexes **11a** and **11b** exhibit one signal each at δ = –57.1 and –56.3, respectively. The central fulvalene C–C bond length of 1.471(6) Å is within the normal range found in fulvalene metal complexes with a degree of multiple bonding between the rings.[50] The bond lengths and angles of the binuclear compound **11b** are similar to those of the analogous mononuclear compound **10b**. The P···Zr distance of 3.0698(9) Å for **11b** is slightly larger than that of 3.0523(6) Å for **10b**.

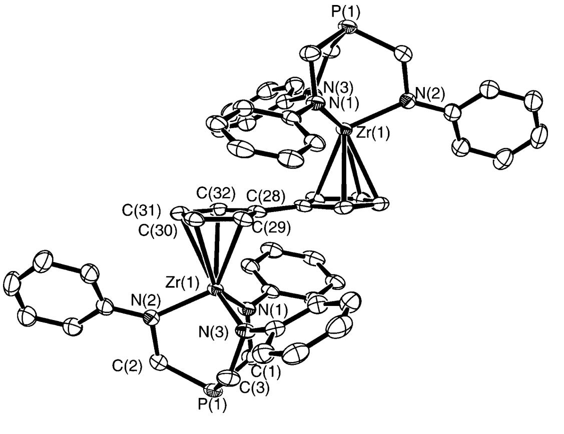

Figure 6. Solid-state molecular structure of **11b** as determined by X-ray crystallography. Ellipsoids are shown at the 50% probability level. Hydrogen atoms and 3,5-methyl substituents are omitted for clarity. Selected distances [Å]: P(1)–Zr(1) 3.0698(9), C(28)–Zr(1) 2.620(3), C(29)–Zr(1) 2.544(3), C(30)–Zr(1) 2.487(3), C(31)–Zr(1) 2.488(3), C(32)–Zr(1) 2.539(3),C(28)-(C28) 1.471(6), C(28)–C(29) 1.414(4), C(29)–C(30) 1.408(4), C(30)–C(31) 1.410(4), C(31)–C(32) 1.407(4), C(28)–C(32) 1.418(4), N(1)–Zr(1) 2.052(2), N(2)–Zr(1) 2.093(3), N(3)–Zr(1) 2.073(3).

In the ^{1}H NMR spectra of *trans*-[P(CH$_2$NAr^R)$_3$Zr]$_2$-(η^5:η^5-C$_{10}$H$_8$) (**11a**,**b**), the fulvalene protons consist of a pair of resonances that appear to be triplets for this AA′BB′ spin system, consistent with the high symmetry of this complex. A significant change of the ^{31}P NMR chemical shift to lower field is observed for complexes **11a** (δ = –57.1 ppm) and **11b** (δ = –56.3 ppm), compared to their corresponding mononuclear zirconium complexes **10a** (δ = –67.5 ppm) and **10b** (δ = –66.9 ppm).

Polymer Synthesis

The bridged binuclear complexes we have prepared should provide a facile route to polymeric materials that contain transition metals along the main polymer chain. The synthetic viability of this approach can be demonstrated using complex **6a**. We have previously shown that two equivalents of the mononuclear complexes P(CH$_2$NAr^R)TiNMe$_2$ (**3a**,**b**) react cleanly with [Rh(CO)$_2$-(μ-Cl)]$_2$ to generate the heterobimetallic complexes *trans*-Cl(CO)Rh[P(CH$_2$NAr^R)$_3$TiNMe$_2$]$_2$.[12] An analogous reaction with one equivalent of the dinuclear oxo-bridged titanium complex **6a** precipitated a red insoluble polymer that analyses as Cl(CO)Rh[P(CH$_2$NPh)$_3$Ti]$_2$O, as shown in Equation (6). A single CO stretch is observed in the IR spectrum of a KBr pellet of **12a** at 1975.2 cm^{-1}. Further work in the preparation of a series of polymers and their complete characterization is currently underway.

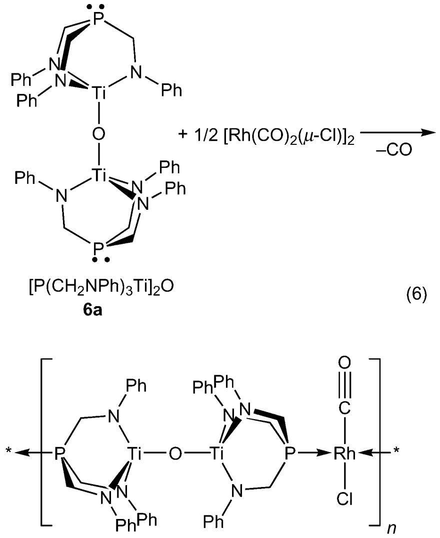

12a

Conclusions

The design of divergent metal-containing building blocks provides a facile route to linear rigid metal-containing polymers. With the smaller metal Ti it proved possible to generate bridges with η^1-bound ligands, whereas with the larger metal Zr attempts to generate bridged complexes only succeeded by utilizing polyhapto ligands. Our future goals include the inclusion of redox active or paramagnetic metal–ligand fragments in lieu of Ti and Zr in the bisphosphane moiety, as well as an in-depth investigation into the properties and characteristics of these polymers and the use of these building blocks in the assembly of higher-dimensional networks with functional physical properties.

Experimental Section

General Procedures: Unless otherwise stated, all manipulations were performed under an inert atmosphere of nitrogen using either standard Schlenk techniques or an M. Braun glove box. Dry, oxygen-free solvents were employed throughout. Anhydrous pentane, toluene, diethyl ether and THF were purchased from Aldrich, sparged with dinitrogen, and passed through activated alumina under a positive pressure of nitrogen gas; toluene and hexanes were further deoxygenated using Ridox catalyst columns.[51] Deuterated benzene, toluene, and THF were dried by heating at reflux with sodium/potassium alloy, sodium, and potassium, respectively, in a sealed vessel under partial pressure, then trap-to-trap distilled, and freeze-pump-thaw degassed three times. Deuterated dichloromethane was heated in a sealed vessel over CaH_2, then trap-to-trap distilled, and freeze-pump-thaw degassed three times. NMR spectra were recorded on Bruker AMX (300 MHz) or Bruker AMX (500 MHz) spectrometer. All chemical shifts are reported in ppm, and all coupling constants are in Hz. For $^{19}F\{^1H\}$ NMR spectra, trifluoroacetic acid was used as the external reference at δ = 0.00 ppm. ^1H NMR spectra were referenced to residual protons (C_6D_5H, δ = 7.15; C_7D_7H, δ = 2.09 ppm) with respect to tetramethylsilane at δ = 0.00 ppm. $^{31}P\{^1H\}$ NMR spectra were referenced to external 85% H_3PO_4 at δ = 0.0. $^{13}C\{^1H\}$ spectra were referenced relative to solvent resonances (C_6D_6, δ = 128.0; C_7D_8, δ = 20.4 ppm). Elemental analyses were performed by the Centre for Catalysis and Materials Research (CCMR), Windsor, Ontario, Canada. The compounds $TiCl_4$, $ZrCl_4(THF)_2$, HO-(4-*t*BuC_6H_3), 4,4′-HO[3,3′,5,5′-$(Me_2C_6H_2)_2$]OH, $HNEt_3Cl$, $(C_5H_5)Li$, $CpZrCl_3$, $[(CO)_2Rh(\mu\text{-}Cl)]_2$, and 1.6 M *n*BuLi in hexanes were purchased from Aldrich, and used as received. The compounds **1a**–**b**,[12] **3a**–**b**,[12] $Ti(NMe_2)_3Cl$,[52] $Zr(NEt_2)_4$,[53] and $(C_{10}H_8)Li_2$,[48] were prepared by published procedures.

$P(CH_2NPh)_3Li_3{\cdot}(Et_2O)_{1.5}$ (2a) and $P(CH_2NPh)_3Li_3(THF)_5$ (2a-THF): A 1.6 M solution of *n*BuLi (28.0 mL, 17.5 mmol, 3 equiv.) in hexanes was added dropwise to a stirred slurry of $P(CH_2NPh)_3H_3$ (2.04 g, 5.84 mmol) in diethyl ether (80 mL) at 0 °C. After the addition of 2 equiv. of *n*BuLi the solution was clear. The addition of the third equivalent precipitated a white solid. The solid was filtered and dried under vacuum (2.17 g, 78%). The product is insoluble in toluene, ether, or CH_2Cl_2. The addition of THF generates the more soluble THF adduct. This adduct is soluble in THF and CH_2Cl_2 but decomposes within an hour at room temperature in the latter. Crystals of the THF adduct suitable for characterization by X-ray diffraction were obtained from THF by slow evaporation. ^1H NMR ([D$_8$]THF, 500.1 MHz, 298 K): δ = 1.12 (t, ^3J = 7.0 Hz, 9 H, OCH_2CH_3) 3.39 (q, ^3J = 7.0 Hz, 6 H, OCH_2CH_3), 3.47 (d, $^2J_{PC}$ = 7.0 Hz, 6 H, PCH_2), 6.09 (t, 3 H, Ph *p-H*), 6.42 (d, $^3J_{HH}$ = 8.3 Hz, 6 H, Ph *o-H*), 6.85 (m, 6 H, Ph *m-H*) ppm. $^{31}P\{^1H\}$ NMR ([D$_8$]THF, 202.5 MHz, 298 K): δ = –22.15 (s) ppm. $^{13}C\{^1H\}$ NMR ([D$_8$]THF, 125.8 MHz, 298 K): δ = 15.9 (s, OCH_2CH_3), 50.3 (d, J_{PC} = 12 Hz, PCH_2), 110.9, 114.2, 129.3 (s, *o,m,p*-Ph), 164.2 (m, *ipso*-C) ppm. ^7Li NMR ([D$_8$]THF, 116.7 MHz, 298 K): δ = 1.34 (s) ppm. $C_{27}H_{36}Li_3N_3O_{1.5}P$ (478.39): calcd. C 67.79, H 7.58, N 8.78; found C 68.08, H 7.49, N 8.74.

$P(CH_2N\text{-}3,5\text{-}Me_2C_6H_3)_3Li_3(Et_2O)_{1.5}$ (2b): A 1.6 M solution of *n*BuLi (9.4 mL, 15 mmol) in hexanes was added dropwise to a stirred slurry of $P(CH_2NH\text{-}3,5\text{-}Me_2C_6H_3)_3$ (2.15 g, 5 mmol) in diethyl ether (50 mL) at 0 °C and stirred at room temperature for 1 h. The resultant solid was filtered and dried under vacuum (2.12 g, 75%). ^1H NMR ([D$_8$]THF, 500.1 MHz, 298 K): δ = 1.11 (t, ^3J = 6.9 Hz, 9 H, OCH_2CH_3), 2.08 (s, 18 H, ArCH_3), 3.38 (m, ^3J = 7.0 Hz, 6 H, OCH_2CH_3 & PCH_2), 5.80 (s, 3 H, *p-H*), 6.10 (s, 6 H, *o-H*) ppm. $^{31}P\{^1H\}$ NMR ([D$_8$]THF, 202.5 MHz, 298 K): δ = –21.7 (s) ppm. $^{13}C\{^1H\}$ NMR ([D$_8$]THF, 125.8 MHz, 298 K): δ = 15.6 (s, OCH_2CH_3), 22.1 (s, PhCH_3), 50.1 (d, J_{PC} = 11 Hz, PCH_2), 66.3 (s, OCH_2CH_3), 112.0, 112.8, 137.3 (s, *o,m,p*-Ph), 164.2 (m, *ipso*-C) ppm. ^7Li NMR ([D$_8$]THF, 116.7 MHz, 298 K): δ = 1.06 (s) ppm. $C_{33}H_{48}Li_3N_3O_{1.5}P$ (562.55): calcd. C 70.46, H 8.60, N 7.47; found C 70.70, H 8.78, N 7.36.

$P(CH_2NPh)_3TiO\text{-}4\text{-}t BuC_6H_3$ (4a): HO(4-*t*BuC_6H_3) (150 mg, 1.0 mmol) were added to a solution of $P(CH_2NPh)_3TiNMe_2$ (**3a**), (438.3 mg, 1.0 mmol) in 50 mL of toluene. The solution was stirred for 48 h. The solvent was removed under vacuum and the remaining red solid was rinsed with a small portion of cold pentane, and then dried under vacuum (277 mg, 51%). ^1H NMR (C_6D_6, 300 MHz, 298 K): δ = 1.19 [s, 9 H, $C(CH_3)_3$], 3.85 (d, $^2J_{PH}$ = 7.0 Hz, 6 H, PCH_2), 6.81 (m, 3 H, Ph *p-H*), 7.04 (m, 2 H, C_6H_4), 7.06 (m, 6 H, Ph *m-H*), 7.13 (m, 2 H, C_6H_4), 7.18 (m, 6 H, Ph *o-H*) ppm. $^{13}C\{^1H\}$ NMR (C_6D_6, 125.8 MHz, 298 K): δ = 1.35 [s, $C(CH_3)_3$], 31.7 [s, $C(CH_3)_3$], 44.1 (d, J_{PC} = 20.0 Hz, PCH_2), 116.4, 119.8, 121.1, 127.0, 129.8, 146.5, and 153.3 (s, C_6H_5, C_6H_4), 164.2 (s, *ipso-C*) ppm. $^{31}P\{^1H\}$ NMR (C_6D_6, 202.5 MHz, 298 K): δ = –81.1 (s) ppm. $C_{31}H_{34}N_3OPTi$ (543.46): calcd. C 68.51, H 6.31, N 7.73; found C 68.92, H 6.85, N 7.27.

$P(CH_2N\text{-}3,5\text{-}Me_2C_6H_3)_3TiOC_6H_3\text{-}4\text{-}t Bu$ (4b): HOC_6H_3-4-*t*Bu (150 mg, 1.0 mmol) were added to a solution of $P(CH_2N\text{-}3,5\text{-}Me_2C_6H_3)_3TiNMe_2$ (**3b**), (522.3 mg, 1.0 mmol) in 50 mL of toluene. The solution was stirred for 48 h. The solvent was removed under vacuum and the remaining red solid was rinsed with a small portion of cold pentane, and then dried under vacuum (378 mg, 60%). X-ray quality crystals were obtained from toluene by slow evaporation. ^1H NMR (C_6D_6, 300 MHz, 298 K): δ = 0.29 [s, 9 H, $C(CH_3)_3$], 1.90 (s, 18 H, ArCH_3), 3.97 (d, $^2J_{PH}$ = 6.8 Hz, 6 H, PCH_2), 6.23 (m, 2 H, C_6H_4), 6.25 (s, 3 H, Ph *p-H*), 6.45 (m, 2 H, C_6H_4), 6.59 (s, 6 H, Ph *o-H*) ppm. $^{13}C\{^1H\}$ NMR (C_6D_6, 125.8 MHz, 298 K): δ = 1.7 [s, $C(CH_3)_3$], 21.3 (s, ArCH_3), 21.9 [s, $C(CH_3)_3$], 45.3 (d, J_{PC} = 18.4 Hz, PCH_2), 112.0, 114.2, 116.0, 116.5, 120.8, 123.5, and 138.6 (s, C_6H_5, C_6H_4), 153.3 (s, *ipso-C*) ppm. $^{31}P\{^1H\}$ NMR (C_6D_6, 202.5 MHz, 298 K): δ = –77.9 (s) ppm. $C_{37}H_{46}N_3OPTi$ (627.62): calcd. C 70.81, H 7.39, N 6.70; found C 69.59, H 7.61, N 6.99.

$[P(CH_2NPh)_3Ti]_2\text{-}[\mu\text{-}4,4'\text{-}O\text{-}3,3',5,5'\text{-}(Me_2C_6H_2)_2O\text{-}]$ (5a): 4,4′-HO[3,3′,5,5′-$(Me_2C_6H_2)_2$]OH (121 mg, 0.5 mmol) was added to a solution of $P(CH_2NPh)_3TiNMe_2$ (438.3 mg, 1.0 mmol) in 50 mL of toluene. The solution was stirred for 48 h. The solvent was removed under vacuum and the remaining red solid was rinsed with a small portion of cold pentane, and then dried under vacuum (277 mg, 51%). ^1H NMR (C_6D_6, 300 MHz, 298 K): δ = 2.24 [s, 12 H, $C_6H_2(CH_3)_2$], 3.93 (d, $^2J_{PH}$ = 7.0 Hz, 12 H, PCH_2), 6.73 (m, 6 H, Ph *p-H*), 6.95 (d, J_{HH} = 8.3 Hz, 6 H, Ph *m-H*), 7.10 (m, 2 H, C_6H_4), 7.17 (s, 4 H, C_6H_2) ppm. $^{13}C\{^1H\}$ NMR (C_6D_6, 125.8 MHz, 298 K): δ = 18.4 [s, $C_6H_2(CH_3)_2$], 45.6 (d, J_{PC} = 20.7 Hz, PCH_2), 113.8, 117.0, 121.5, 127.7, 129.5, and 135.7 (s, C_6H_5, C_6H_2), 153.9 (s, *ipso*-C_6H_5), 164.2 (s, *ipso*-O-C_6H_2) ppm. $^{31}P\{^1H\}$ NMR (C_6D_6, 202.5 MHz, 298 K): δ = –78.6 (s) ppm. $C_{58}H_{58}N_6O_2P_2Ti_2$ (1028.80): calcd. C 67.71, H 5.68, N 8.17; found C 67.37, H 5.58, N 7.89.

$[P(CH_2NPh)_3Ti]_2(\mu\text{-}O)$ (6a): Solid $Na_2SO_4{\cdot}10H_2O$ (16.1 mg, 0.5 mmol H_2O) was added to $P(CH_2NPh)_3TiNMe_2$ (438.3 mg, 1.0 mmol) dissolved in 50 mL of toluene and 10 mL of THF. The solution was stirred for two weeks. The solvent was removed under vacuum and the remaining red solid was rinsed with a small portion of cold pentane, and then dried under vacuum (200 mg, 49%). X-ray quality crystals were obtained by recrystallization from toluene; both trigonal and a monoclinic pseudopolymorphs were identified by X-ray crystallography. ^{1}H NMR (C_6D_6, 300 MHz, 298 K): δ = 3.68 (d, $^{2}J_{PH}$ = 7.8 Hz, 12 H, PC*H*$_2$), 6.68 (t, *J* = 7.3 Hz, 6 H, Ph *p-H*), 6.80 (d, *J* = 8.2 Hz, 6 H, Ph *o-H*), 6.92 (t, *J* = 7.8 Hz, 6 H, Ph *m-H*) ppm. ^{13}C{^{1}H} NMR (C_6D_6, 125.8 MHz, 298 K): δ = 45.4 (d, J_{PC} = 19.8 Hz, P*C*H$_2$), 117.2, 121.6 and 129.4 (s, *C*$_6$H$_5$), 153.8 (s, *ipso-C*) ppm. ^{31}P{^{1}H} NMR (C_6D_6, 202.5 MHz, 298 K): δ = –39.3 (s) ppm. $C_{42}H_{42}N_6OP_2Ti_2$ (804.50): calcd. C 62.70, H 5.26, N 10.45; found C 62.40, H 5.14, N 10.52.

$P(CH_2N\text{-}3,5\text{-}Me_2C_6H_3)_3Ti\text{-}\mu\text{-}O\text{-}Ti(NMe_2)_3$ (7b): $Ti(NMe_2)_4$ (224.2 mg, 1.0 mmol) and a 1.0 M solution of H_2O in diethyl ether (1.0 mL, 1.0 mmol) were added to a solution of $P(CH_2N\text{-}3,5\text{-}Me_2C_6H_3)_3TiNMe_2$ (522.3 mg, 1.0 mmol) in 50 mL of toluene. The solution was stirred for 24 h and the solvents evaporated to dryness, then 5 mL of pentane and 10 mL of hexamethyldisiloxane were added. The solution was filtered and the remaining orange red solid was rinsed with a small portion of cold pentane, and then dried under vacuum (370 mg, 55%). X-ray quality crystals were grown from toluene. ^{1}H NMR (C_6D_6, 500 MHz, 298 K): δ = 2.27 (s, 18 H, ArC*H*$_3$), 3.03 (s, 18 H, N*Me*$_2$), 3.84 (d, $^{2}J_{PH}$ = 7.0 Hz, 6 H, PC*H*$_2$), 6.60 (s, 6 H, Ph *o-H*), 6.87 (s, 3 H, Ph *p-H*) ppm. ^{13}C{^{1}H} NMR (C_6D_6, 125.8 MHz, 298 K): δ = 22.1 (s, Ar*C*H$_3$), 44.3 (s, N*Me*$_2$), 44.8 (d, J_{PC} = 19.7 Hz, P*C*H$_2$), 114.5, 122.2, and 138.3 (s, Ph *o-C*, *m-C* and *p-C*), 153.8 (s, *ipso-C*) ppm. ^{31}P{^{1}H} NMR (C_6D_6, 202.5 MHz, 298 K): δ = –62.9 (s) ppm. $C_{33}H_{51}N_6OPTi_2$ (674.51): calcd. C 58.76, H 7.62, N 12.46; found C 58.59, H 7.41, N 11.99.

$P(CH_2NPh)_3ZrNEt_2$ (8a): Liquid $Zr(NEt_2)_4$ (3.246 g, 8.55 mmol) was added to a solution of $P(CH_2NHPh)_3$ (2.987 g, 8.55 mmol) in 30 mL of toluene. The pale yellow solution was stirred 24 h. The solvent was removed under vacuum and the remaining yellow solid was rinsed with a small portion of pentane, and then dried under vacuum (3.76 g, 86%). The product has only moderate solubility in benzene at room temperature, but is quite soluble in hot benzene. ^{1}H NMR (C_6D_6, 300 MHz, 298 K): δ = 1.01 (t, ^{3}J = 7.0 Hz, 6 H, NCH$_2$C*H*$_3$), 3.20 (q, ^{3}J = 7.0 Hz, 4 H, NC*H*$_2$CH$_3$), 3.83 (d, $^{2}J_{PH}$ = 6.4 Hz, 6 H, PC*H*$_2$), 6.80 (d, 6 H, Ph *o-H*), 6.85 (t, 3 H, Ph *p-H*), 7.23 (m, 6 H, Ph *m-H*) ppm. ^{13}C{^{1}H} NMR (C_6D_6, 125.8 MHz, 298 K): δ = 14.5 (s, NCH$_2$*C*H$_3$), 42.8 (s, ZrN*C*H$_2$CH$_3$), 44.5 (d, J_{PC} = 23 Hz, P*C*H$_2$), 117.8 and 129.7 (s, Ph *o-C* and *m-C*), 120.2 (s, Ph *p-C*), 153.6 (d, *ipso-C*) ppm. ^{31}P{^{1}H} NMR (C_6D_6, 121.5 MHz, 298 K): δ = –75.2 (s) ppm. $C_{25}H_{31}N_4PZr$ (509.74): calcd. C 58.91, H 6.13, N 10.99; found C 58.55, H 6.17, N 10.77.

$P(CH_2N\text{-}3,5\text{-}Me_2C_6H_3)_3ZrNEt_2$ (8b): Liquid $Zr(NEt_2)_4$ (3.79 g, 10.0 mmol) was added to a solution of $P(CH_2NH\text{-}3,5\text{-}Me_2C_6H_3)_3$ (4.30 g, 10.0 mmol) in 50 mL of toluene. The pale yellow solution was stirred 48 h. The solvent was removed under vacuum and the remaining yellow solid was rinsed with a small portion of pentane, and then dried under vacuum (4.12 g, 69.4%) The product has only moderate solubility in benzene at room temperature, but is quite soluble in hot benzene. ^{1}H NMR (C_6D_6, 300 MHz, 298 K): δ = 1.12 (t, ^{3}J = 7.1 Hz, 6 H, NCH$_2$C*H*$_3$), 2.23 (s, 18 H, PhC*H*$_3$), 3.37 (q, ^{3}J = 7.1 Hz, 4 H, NC*H*$_2$CH$_3$), 3.95 (d, $^{2}J_{PH}$ = 6.8 Hz, 6 H, PC*H*$_2$), 6.52 (s, 6 H, Ph *o*-H), 6.55 (s, 3 H, Ph *p*-H) ppm. ^{13}C{^{1}H} NMR (C_6D_6, 125.8 MHz, 298 K): δ = 14.6 (s, NCH$_2$*C*H$_3$), 22.1 (s, Ph*C*H$_3$), 42.8 (s, ZrN*C*H$_2$CH$_3$), 44.9 (d, J_{PC} = 22.0 Hz, P*C*H$_2$), 115.9 and 122.2 (s, Ph *o-C* and *m-C*), 138.9 (s, Ph *p-C*), 153.8 (d, J_{CC} = 2.7 Hz, *ipso-C*) ppm. ^{31}P{^{1}H} NMR (C_6D_6, 121.5 MHz, 298 K): δ = –70.8 (s) ppm. $C_{31}H_{43}N_4PZr$ (593.90): calcd. C 62.69, H 7.30, N 9.43; found C 62.50, H 6.99, N 9.12.

$P(CH_2NPh)_3ZrCl(THF)$ (9a): Solid $P(CH_2NPh)_3ZrNEt_2$ (**8a**) (1.17 g, 2.0 mmol) was added to a slurry of $HNEt_3Cl$ (275 mg, 2.0 mmol) in 50 mL of toluene. The pale yellow solution was stirred 1 h, then 5 mL of THF was added. The solvent was removed under vacuum and the remaining yellow solid was rinsed with a small portion of pentane, and then dried under vacuum (0.91 g, 84.1%). ^{1}H NMR (C_6D_6, 300 MHz, 298 K): δ = 0.74 (m, 4 H, OC*H*$_2$), 3.47 (m, 4 H, OCH$_2$C*H*$_2$), 3.81 (d, $^{2}J_{PH}$ = 7.0 Hz, 6 H, PC*H*$_2$), 6.77 (t, 3 H, Ph *p-H*), 6.98 (d, 6 H, Ph *o-H*), 7.16 (m, 6 H, Ph *m-H*) ppm. ^{13}C{^{1}H} NMR (C_6D_6, 125.8 MHz, 298 K): δ = 25.4 (s, O*C*H$_2$), 44.1 (d, J_{PC} = 21 Hz, P*C*H$_2$), 72.8 (s, OCH$_2$*C*H$_2$) 117.8 and 129.5 (s, Ph *o-C* and *m-C*), 120.4 (s, Ph *p-C*), 153.4 (d, *ipso-C*) ppm. ^{31}P{^{1}H} NMR (C_6D_6, 121.5 MHz, 298 K): δ = –71.5 (s) ppm. $C_{25}H_{29}ClN_3OPZr$ (545.17): calcd. C 55.08, H 5.36, N 7.71; found C 54.83, H 5.48, N 8.02.

$P(CH_2N\text{-}3,5\text{-}Me_2C_6H_3)_3ZrCl(THF)$ (9b): Solid $P(CH_2N\text{-}3,5\text{-}Me_2C_6H_3)_3ZrNEt_2$ (**8b**) (2.93 g, 5.0 mmol) was added to a solution of $HNEt_3Cl$ (0.688 g, 5.0 mmol) in 120 mL of toluene. The pale yellow solution was stirred 1 h, then was added 12 mL of THF. The solvent was removed under vacuum and the remaining yellow solid was rinsed with a small portion of pentane, and then dried under vacuum (2.80 g, 90%). ^{1}H NMR (C_6D_6, 300 MHz, 298 K): δ = 0.79 (m, 4 H, OC*H*$_2$), 2.20 (s, 18 H, PhC*H*$_3$), 3.55 (m, 4 H, OCH$_2$C*H*$_2$), 3.92 (d, $^{2}J_{PH}$ = 6.4 Hz, 6 H, PC*H*$_2$), 6.45 (s, 6 H, Ph *o-H*), 6.72 (s, 3 H, Ph *p-H*) ppm. ^{13}C{^{1}H} NMR (C_6D_6, 125.8 MHz, 298 K): δ = 21.7 (s, Ph*C*H$_3$), 25.1 (s, O*C*H$_2$), 44.1 (d, J_{PC} = 19.8 Hz, P*C*H$_2$), 72.5 (s, OCH$_2$*C*H$_2$), 115.5 and 122.1 (s, Ph *o-C* and *m-C*), 138.2 (s, Ph *p-C*), 153.1 (d, J_{CC} = 2.7 Hz, *ipso-C*) ppm. ^{31}P{^{1}H} NMR (C_6D_6, 121.5 MHz, 298 K): δ = –66.0 (s) ppm. $C_{31}H_{41}ClN_3OPZr$ (629.33): calcd. C 59.16, H 6.57, N 6.68; found C 59.12, H 6.29, N 6.79.

$P(CH_2NPh)_3ZrCp$ (10a): Solid $P(CH_2NPh)_3ZrCl(THF)$ (**9a**) (545.17 mg, 1.0 mmol) was added to a solution of CpLi (72.03 mg, 1.0 mmol) in 50 mL of toluene. The yellow solution was stirred 20 h. The solvent was removed under vacuum and the remaining yellow solid was rinsed with a small portion of pentane, and then dried under vacuum (420 mg, 80%). ^{1}H NMR (C_6D_6, 300 MHz, 298 K): δ = 3.90 (d, $^{2}J_{PH}$ = 7.3 Hz, 6 H, PC*H*$_2$), 5.95 (s, 5 H, C$_5$*H*$_5$), 6.85 (d, 6 H, Ph *o-H*), 6.92 (t, 3 H, Ph *p-H*), 7.20 (m, 6 H, Ph *m-H*) ppm. ^{13}C{^{1}H} NMR (C_6D_6, 125.8 MHz, 298 K): δ = 46.8 (d, J_{PC} = 23.1 Hz, P*C*H$_2$), 72.8 (s, THF), 114.6, 121.9, 122.8, 129.3 (s, Ph *o-C*, *m-C*, *p-C*, *C*$_5$H$_5$), 153.4 (s, *ipso-C*) ppm. ^{31}P{^{1}H} NMR (C_6D_6, 121.5 MHz, 298 K): δ = –67.5 (s) ppm. $C_{26}H_{26}N_3PZr$ (502.70): calcd. C 62.12, H 5.21, N 8.36; found C 62.37, H 5.48, N 8.02.

$P(CH_2N\text{-}3,5\text{-}Me_2C_6H_3)_3ZrCp$ (10b): Solid $P(CH_2N\text{-}3,5\text{-}Me_2C_6H_3)_3ZrCl(THF)$ (**9b**) (629.33 mg, 1.0 mmol) was added to a solution of CpLi (72.03 mg, 1.0 mmol) in 50 mL of toluene. The yellow solution was stirred 20 h. The solvent was removed under vacuum and the remaining yellow solid was rinsed with a small portion of pentane, and then dried under vacuum (530 mg, 90%). X-ray quality crystals were obtained from slow evaporation of a toluene solution. ^{1}H NMR (C_6D_6, 300 MHz, 298 K): δ = 2.23 (s, 18 H, PhC*H*$_3$), 4.00 (d, $^{2}J_{PH}$ = 6.7 Hz, 6 H, PC*H*$_2$), 6.18 (s, 5 H, C$_5$*H*$_5$), 6.60 (s, 3 H, Ph *p-H*), 6.68 (s, 6 H, Ph *o-H*) ppm. ^{13}C{^{1}H} NMR (C_6D_6, 125.8 MHz, 298 K): δ = 21.8 (s, Ph*C*H$_3$), 47.0 (d, J_{PC} = 23.1 Hz, P*C*H$_2$), 114.6, 120.8, 123.8, 138.4 (s, Ph *o-C*, *m-C*, *p-C*, *C*$_5$H$_5$), 159.9 (s, *ipso-C*) ppm. ^{31}P{^{1}H} NMR (C_6D_6, 121.5 MHz, 298 K): δ = –66.9 (s) ppm. $C_{32}H_{38}N_3PZr$ (586.86): calcd. C 65.49, H 6.53, N 7.16; found C 65.68, H 6.64, N 6.69.

[P(CH$_2$NPh)$_3$Zr]$_2$(η^5:η^5-C$_{10}$H$_8$) (11a): Solid P(CH$_2$NPh)$_3$-ZrCl(THF) (**9a**) (545.17 mg, 1.0 mmol) was added to a solution of (C$_{10}$H$_8$)Li$_2$[48] (72 mg, 0.5 mmol) in 50 mL of toluene. The solution was stirred 12 h and filtered to remove the solid. The solvent was removed under vacuum and the remaining yellow solid was rinsed with a small portion of pentane, and then dried under vacuum (205 mg, 40 %). ^{1}H NMR (C$_6$D$_6$, 300 MHz, 298 K): δ = 3.89 (d, $^2J_{PH}$ = 7.3 Hz, 12 H, PC*H*$_2$), 5.49 (s, 4 H, C$_{10}$*H*$_8$), 5.93 (s, 4 H, C$_{10}$*H*$_8$), 6.70 (d, 6 H, Ph *o-H*), 6.90 (t, 3 H, Ph *p-H*), 7.20 (m, 6 H, Ph *m-H*) ppm. ^{13}C{^{1}H} NMR (C$_6$D$_6$, 125.8 MHz, 298 K): δ = 46.9 (d, J_{PC} = 23.0 Hz, PCH$_2$), 113.9 and 118.8, 123.1, 129.2, 129.8, 138.9 (s, Ph *o-C*, *m-C*, *p-C*, *C*$_{10}$H$_8$), 158.8 (s, *ipso-C*) ppm. ^{31}P{^{1}H} NMR (C$_6$D$_6$, 121.5 MHz, 298 K): δ = –57.1 (s) ppm. (C$_{26}$H$_{26}$N$_3$PZr)$_2$ (1005.4): calcd. C 62.12, H 5.21, N 8.36; found C 61.79, H 5.64, N 8.47.

[P(CH$_2$N-3,5-Me$_2$C$_6$H$_3$)$_3$Zr]$_2$(η^5:η^5-C$_{10}$H$_8$) (11b): P(CH$_2$N-3,5-Me$_2$C$_6$H$_3$)$_3$ZrCl(THF) (**9b**) (629.33 mg, 1.0 mmol) was added to a solution of (C$_{10}$H$_8$)Li$_2$[48] (72 mg, 0.5 mmol) in 50 mL of toluene. The solution was stirred 12 h and filtered to remove the solid. The solvent was removed under vacuum and the remaining yellow solid was rinsed with a small portion of pentane, and then dried under vacuum (280 mg, 48 %). X-ray quality crystals were obtained from slow evaporation of a mixture of benzene and hexamethyldisilox-

Table 1. Crystallographic data and structure refinement for **2a-THF**, **4b**, **6a**, **7b**, **10b** and **11b**.

	2a-THF	**4b**	**6a**	**6a**
Empirical formula	C$_{41}$H$_{61}$Li$_3$N$_3$O$_5$P	C$_{37}$H$_{46}$N$_3$OPTi·0.5(C$_5$H$_{12}$)	C$_{42}$H$_{42}$N$_6$OP$_2$Ti$_2$	C$_{49}$H$_{50}$N$_6$OP$_2$Ti$_2$
Formula weight	727.72	663.71	804.56	896.69
Crystal system	orthorhombic	triclinic	trigonal	monoclinic
a [Å]	25.863(14)	14.225(3)	13.0770(14)	23.062(2)
b [Å]	14.907(8)	14.471(3)	13.0770(14)	10.0301(10)
c [Å]	10.978(6)	20.351(5)	20.452(4)	19.319(2)
α [°]	90	71.232(3)	90	90
β [°]	90	77.687(3)	90	90.8680(10)
γ [°]	90	68.183(3)	120	90
V [Å^3]	4232(4)	3661.6(14)	3028.8(8)	4468.3(8)
Space group	*Pna*21	*P*-1	*R*-3	*Pc*
Z value	4	4	3	4
$D_{calcd.}$ [g/cm^3]	1.142	1.204	1.323	1.333
μ (Mo-K_α) [mm^{-1}]	0.108	0.311	0.515	0.473
Temperature [K]	293(2)K	173(2)	173(2)	173(2)
$2\theta_{max}$ [°]	50.0	50.0	55.0	55.0
Total number of reflections	17447	35194	11068	48484
Unique reflections, R_{int}	6005; 0.0413	12848; 0.0538	1548; 0.0496	19725; 0.0323
Transmission factors	0.94–0.98	0.89–0.98	0.86–0.90	0.80–0.83
Reflections with $I \geq 2\sigma(I)$	3834	9800	1356	18481
Number of variables	471	825	81	1083
Reflections/parameters	12.7	15.6	19.1	18.2
R; *wR*$_2$ (all data)	0.078; 0.142	0.1008; 0.1790	0.0709; 0.1351	0.0625; 0.1398
GOF	0.919	1.130	1.195	1.162
Residual density [e$^-$/Å^3]	0.421, –0.196	0.667, –0.548	0.561, –0.437	0.703, –0.527

	7b	**10b**	**11b**
Empirical formula	C$_{33}$H$_{51}$N$_6$OPTi$_2$	C$_{32}$H$_{38}$N$_3$PZr	C$_{76}$H$_{86}$N$_6$P$_2$Zr$_2$
Formula weight	674.57	586.84	1327.89
Crystal system	trigonal	triclinic	monoclinic
a [Å]	15.861(2)	11.4611(9)	15.120(2)
b [Å]	15.861(2)	15.4190(12)	13.8406(19)
c [Å]	24.504(7)	18.5870(14)	18.128(3)
α [°]	90	101.2880(10)	90
β [°]	90	107.8600(10)	113.6850(10)
γ [°]	120	102.3990(10)	90
V [Å^3]	5339(2)	2930.1(4)	3474.2(8)
Space group	*R*-3	*P*-1	*P*2$_1$/*n*
Z value	6	4	2
$D_{calcd.}$ [g/cm^3]	1.259	1.330	1.269
μ (Mo-K_α) [mm^{-1}]	0.527	0.455	0.392
Temperature [K]	173(2)	173(2)	173(2)
$2\theta_{max}$ [°]	55.0	50.0	55.0
Total number of reflections	16998	28289	37628
Unique reflections, R_{int}	2667; 0.0820	10288; 0.0208	7869; 0.0473
Transmission factors	0.88–0.91	0.67–0.85	0.92–0.99
Reflections with $I \geq 2\sigma(I)$	1808	9362	6849
Number of variables	134	679	394
Reflections/parameters	19.9	15.2	20.0
R; *wR*$_2$ (all data)	0.0790; 0.1533	0.0331; 0.0785	0.0661; 0.1191
GOF	1.057	1.054	1.210
Residual density [e$^-$/Å^3]	0.539, –0.599	0.390, –0.260	0.785, –0.660

ane solution. ^{1}H NMR (C_6D_6, 300 MHz, 298 K): δ = 2.18 (s, 36 H, PhCH_3), 3.86 (d, $^2J_{PH}$ = 7.2 Hz, 12 H, PCH_2), 5.70 (s, 4 H, $C_{10}H_8$), 6.17 (s, 4 H, $C_{10}H_8$), 6.50 (s, 6 H, Ph *o-H*), 6.55 (s, 3 H, Ph *p-H*) ppm. ^{13}C{^{1}H} NMR (C_6D_6, 125.8 MHz, 298 K): δ = 21.8 (s, PhCH_3), 48.1 (d, J_{PC} = 22.2 Hz, PCH_2), 112.6 and 121.8, 124.0, 138.2 (s, Ph *o-C*, *m-C*, *p-C*, $C_{10}H_8$), 158.9 (s, *ipso-C*) ppm. ^{31}P{^{1}H} NMR (C_6D_6, 121.5 MHz, 298 K): δ = –56.3 (s) ppm. $(C_{32}H_{38}N_3PZr)_2$ (1173.72): calcd. C 65.49, H 6.53, N 7.16; found C 65.76, H 6.83, N 7.53.

Cl(CO)Rh[P(CH$_2$NPh)$_3$Ti]$_2$O (12a): The dinuclear oxo-bridged titanium complex **6a** (64.4 mg, 0.08 mmol) was added to a solution of $[(CO)_2Rh(\mu\text{-}Cl)]_2$ (15.5 mg, 0.5 equiv.). Within minutes a red insoluble polymer begins to precipitate. The solution was stirred overnight, filtered and the insoluble red solid dried under vacuum (67 mg, 87%). IR (KBr pellet): $\tilde{\nu}$ = 1975.2 cm^{-1}. $C_{43}H_{42}ClN_6O_2P_2RhTi_2$ (970.87): calcd. C 53.20, H 4.36, N 8.66; found C 52.78, H 4.41, N 8.41.

X-ray Crystallography: The X-ray structures were obtained at low temperature, with each crystal covered in Paratone and placed rapidly into the cold N_2 stream of the Kryo-Flex low-temperature device. The data were collected using the SMART[54] software with a Bruker APEX CCD diffractometer using a graphite monochromator with Mo-K_α radiation (λ = 0.71073 Å). A hemisphere of data was collected using a counting time of 10 to 30 s per frame. Details of crystal data, data collection, and structure refinement are listed in Table 1. Data reductions were performed using the SAINT[55] software, and the data were corrected for absorption using SADABS.[56] The structures were solved by direct methods using SIR97[57] and refined by full-matrix least-squares on F^2 with anisotropic displacement parameters for the non-H atoms using SHELXL-97[58] and the WinGX[59] software package. In **2a-THF** one of the THF carbon atoms was modeled as disordered over 2 sites, and thus was refined using isotropic thermal parameters. Complex **4b** crystallized with a disordered pentane molecule in the lattice; the carbon atoms of this moiety were modeled using isotropic thermal parameters. Additionally, one of the *t*Bu substituents exhibited rotational disorder, and two of the carbon atoms associated with this moiety had to be modeled using isotropic thermal parameters. Thermal ellipsoid plots were produced using ORTEP32.[60]

The supplementary crystallographic data for this paper are contained in CCDC-659917 (for **2a-THF**), -659918 (for **4b**), -659919 (for **6a** monoclinic), -659920 (for **6a** triclinic), -659921 (for **7b**), -659922 (for **10b**), -659923 (for **11b**). These data can be obtained free of charge from The Cambridge Crystallographic Data Centre via www.ccdc.cam.ac.uk/data_request/cif.

Acknowledgments

We thank theNational Sciences and Engineering Council (NSERC) of Canada and the Ontario Research and Development Challenge Fund (University of Windsor Centre for Catalysis and Materials Research) for their financial support.

---

[1] A. S. Abd-El-Aziz, I. Manners, *Frontiers in Transition Metal-Containing Polymers*, John Wiley & Sons, Hoboken, **2007**.

[2] F. A. Cotton, C. Lin, C. A. Murillo, *Acc. Chem. Res.* **2001**, *34*, 759–771.

[3] G. F. Swiegers, T. J. Malefetse, *Coord. Chem. Rev.* **2002**, *225*, 91–121.

[4] S. A. Barnett, N. R. Champness, *Coord. Chem. Rev.* **2003**, *246*, 145–168.

[5] P. J. Steel, *Acc. Chem. Res.* **2005**, *38*, 243–250.

[6] S. R. Seidel, P. J. Stang, *Acc. Chem. Res.* **2002**, *35*, 972–983.

[7] S.-S. Sun, A. J. Lees, *Coord. Chem. Rev.* **2002**, *230*, 171–192.

[8] S. Campagna, C. Di Pietro, F. Loiseau, B. Maubert, N. McClenaghan, R. Passalacqua, F. Puntoriero, V. Ricevuto, S. Serroni, *Coord. Chem. Rev.* **2002**, *229*, 67–74.

[9] G. F. Swiegers, T. J. Malefetse, *Chem. Rev.* **2000**, *100*, 3483–3537.

[10] S. Leininger, B. Olenyuk, P. J. Stang, *Chem. Rev.* **2000**, *100*, 853–907.

[11] A. L. Keen, M. Doster, H. Han, S. A. Johnson, *Chem. Commun.* **2006**, 1221–1223.

[12] H. Han, M. Elsmaili, S. A. Johnson, *Inorg. Chem.* **2006**, *45*, 7435–7445.

[13] H. Han, S. A. Johnson, *Organometallics* **2006**, *25*, 5594–5602.

[14] L. H. Gade, *J. Organomet. Chem.* **2002**, *661*, 85–94.

[15] L. Jia, E. Ding, A. L. Rheingold, B. Rhatigan, *Organometallics* **2000**, *19*, 963–965.

[16] L. Turculet, T. D. Tilley, *Organometallics* **2002**, *21*, 3961–3972.

[17] R. Hoffmann, *Acc. Chem. Res.* **1971**, *4*, 1–9.

[18] C. A. Tolman, *Chem. Rev.* **1977**, *77*, 313–348.

[19] R. Raturi, J. Lefebvre, D. B. Leznoff, B. R. McGarvey, S. A. Johnson, *Chem. Eur. J.*; DOI: 10.1002/chem.200700355.

[20] D. W. Stephan, *Coord. Chem. Rev.* **1989**, *95*, 41–107.

[21] N. Wheatley, P. Kalck, *Chem. Rev.* **1999**, *99*, 3379–3419.

[22] P. D. Harvey, *Frontiers in Transition Metal-Containing Polymers 2007*, 321–368.

[23] J. R. Farrell, A. H. Eisenberg, C. A. Mirkin, I. A. Guzei, L. M. Liable-Sands, C. D. Incarvito, A. L. Rheingold, C. L. Stern, *Organometallics* **1999**, *18*, 4856–4868.

[24] A. H. Eisenberg, F. M. Dixon, C. A. Mirkin, C. L. Stern, C. D. Incarvito, A. L. Rheingold, *Organometallics* **2001**, *20*, 2052–2058.

[25] M. C. Alvarez-Vergara, M. A. Casado, M. L. Martin, F. J. Lahoz, L. A. Oro, J. J. Perez-Torrente, *Organometallics* **2005**, *24*, 5929–5936.

[26] G. S. Ferguson, P. T. Wolczanski, *Organometallics* **1985**, *4*, 1601–1605.

[27] R. W. Alder, C. P. Butts, A. G. Orpen, D. Read, J. M. Oliva, *J. Chem. Soc. Perkin Trans. 2* **2001**, 282–287.

[28] R. W. Alder, D. D. Ellis, R. Gleiter, C. J. Harris, H. Lange, A. G. Orpen, D. Read, P. N. Taylor, *J. Chem. Soc. Perkin Trans. 1* **1998**, 1657–1668.

[29] R. W. Alder, D. D. Ellis, A. G. Orpen, P. N. Taylor, *Chem. Commun.* **1996**, 539–540.

[30] B. N. Diel, A. D. Norman, *Phosphorus Sulfur Silicon Relat. Elem.* **1982**, *12*, 227–235.

[31] P. Kisanga, J. Verkade, *Heteroat. Chem.* **2001**, *12*, 114–117.

[32] H. Keller, M. Regitz, *Tetrahedron Lett.* **1988**, *29*, 925–928.

[33] L. H. Gade, N. Mahr, *J. Chem. Soc. Dalton Trans.* **1986**, 489–494.

[34] K. W. Hellmann, L. H. Gade, W.-S. Li, M. McPartlin, *Inorg. Chem.* **1994**, *33*, 5974–5977.

[35] S. Arevalo, M. R. Bonillo, E. De Jesus, F. J. De la Mata, J. C. Flores, R. Gomez, P. Gomez-Sal, P. Ortega, *J. Organomet. Chem.* **2003**, *681*, 228–236.

[36] S. Bieller, M. Bolte, H.-W. Lerner, M. Wagner, *Inorg. Chem.* **2005**, *44*, 9489–9496.

[37] S. Arevalo, J. M. Benito, E. De Jesus, F. J. De la Mata, J. C. Flores, R. Gomez, *J. Organomet. Chem.* **1999**, *592*, 265–270.

[38] A. Kuenzel, M. Sokolow, F.-Q. Liu, H. W. Roesky, M. Noltemeyer, H.-G. Schmidt, I. Uson, *J. Chem. Soc. Dalton Trans.* **1996**, 913–919.

[39] R. Fandos, B. Gallego, A. Otero, A. Rodriguez, M. J. Ruiz, P. Terreros, C. Pastor, *Dalton Trans.* **2006**, 2683–2690.

[40] J. R. Hagadorn, J. Arnold, *J. Am. Chem. Soc.* **1996**, *118*, 893–894.

[41] R. Baumann, R. Stumpf, W. M. Davis, L.-C. Liang, R. R. Schrock, *J. Am. Chem. Soc.* **1999**, *121*, 7822–7836.

[42] A. Ceccon, S. Santi, L. Orian, A. Bisello, *Coord. Chem. Rev.* **2004**, *248*, 683–724.
[43] M.-H. Delville, *Inorg. Chim. Acta* **1999**, *291*, 1–19.
[44] P. A. McGovern, K. P. C. Vollhardt, *Synlett* **1990**, 493–500.
[45] C. G. de Azevedo, K. P. C. Vollhardt, *Synlett* **2002**, 1019–1042.
[46] Y. K. Kang, K. S. Shin, S.-G. Lee, I. S. Lee, Y. K. Chung, *Organometallics* **1999**, *18*, 180–186.
[47] J. H. Davis Jr, E. Sinn, R. N. Grimes, *J. Am. Chem. Soc.* **1989**, *111*, 4784–4790.
[48] C. J. Curtis, R. C. Haltiwanger, *Organometallics* **1991**, *10*, 3220–3226.
[49] C. Moreno, M.-J. Macazaga, R.-M. Medina, D. H. Farrar, S. Delgado, *Organometallics* **1998**, *17*, 3733–3738.
[50] J. S. Drage, K. P. C. Vollhardt, *Organometallics* **1986**, *5*, 280–297.
[51] A. B. Pangborn, M. A. Giardello, R. H. Grubbs, R. K. Rosen, F. J. Timmers, *Organometallics* **1996**, *15*, 1518–1520.
[52] D. G. Dick, R. Rousseau, D. W. Stephan, *Can. J. Chem.* **1991**, *69*, 357–362.
[53] G. M. Diamond, R. F. Jordan, J. L. Petersen, *Organometallics* **1996**, *15*, 4030–4037.
[54] *SMART*, Molecular analysis research tool, Bruker AXS Inc., Madison, WI, **2001**.
[55] *SAINTPlus*, Data reduction and correction program, Bruker AXS Inc., Madison, WI, **2001**.
[56] *SADABS*, An empirical absorption correction program, Bruker AXS Inc., Madison, WI, **2001**.
[57] A. Altomare, M. C. Burla, M. Camalli, G. L. Cascarano, C. Giacovazzo, A. Guagliardi, A. G. G. Moliterni, G. Polidori, R. Spagna, *J. Appl. Crystallogr.* **1999**, *32*, 115–119.
[58] G. M. Sheldrick, *SHELXL-97*, University of Göttingen, Göttingen, **1997**.
[59] L. J. Farrugia, *J. Appl. Crystallogr.* **1999**, *32*, 837–838.
[60] L. J. Farrugia, *J. Appl. Crystallogr.* **1997**, *30*, 565.

Received: September 19, 2007